Property of ECR Process Plasma†

Shoji MIYAKE*, Wei CHEN**, Yoshihiro SHIBATA*** and Tomio ARIYASU****

Abstract

ECR plasma designed for material process by microwave radiation of f = 2.45 GHz was studied experimentally with emphasis on the spatial structure of the plasma. Several magnetic field and chamber configurations were applied and remarkable difference in the plasma parameters and spatial structures was clarified in the hydrogen pressure range of 10^{-2}–10^{-1} Pa. In an appropriate chamber configuration the electron temperature could be controlled from several eV up to 20 eV by changing the incident microwave power and/or magnetic field intensity. Local structure of the resonance zones was varified to give strong influence to the plasma property especially to the spatial distribution of the plasma parameters.

KEY WORDS: (ECR Plasma) (Plasma Process) (Microwave Plasma) (Mirror Field)

1. Introduction

Gaseous plasmas have been successfully applied in new materials synthesis and treatment (plasma CVD, plasma etching and so on). Process plasmas have exhibited high potential in various thin-film synthesis, such as nitriding, oxidation, carburizing and polymerization. Among them an electron cyclotron (ECR) microwave plasma[1–4] has recently been found potentially useful for thin-film process even at low gas pressures of 10^{-1} to 10^{-3} Pa with a lower substrate temperature. This plasma typically reveals following comfortable characteristics: 1) high electron density in the order of 10^{10}–10^{12} cm^{-3}, 2) higher ionization rate of more than several percentages, 3) existence of fast electrons, i.e. high electron temperature, and 4) controllability of electron temperature and electron density in local space. Furthermore many kinds of reactive gas species can be used since ECR plasma is intrinsically electrodeless discharge.

In spite of various successful applications of ECR plasma in material process, information on the plasma parameters and its controllability has not clearly been reported systematically as functions of various external parameters. Especially appropriate control of the local structure and energy distribution of the plasma is considered to be a key problem.

In this paper property of ECR process plasma is reported with emphases on the spatial structure and the control of plasma parameters.

2. Experimental Arrangement

The experimental apparatuses used are shown schematically in **Fig. 1**. We have used three kinds of chambers as shown in 1), 2), and 3) of the figure. The chamber-1 has a symmetric structure with a diameter of 40 cm in the central part over the axial length of z = ±10 cm. The chamber diameter is lowered to 15 cm at two coil regions. The total length of the chamber is 80 cm. In the chamber-2 the diameter of the right side is reduced to 11 cm with a length of only about 10 cm. And in the chamber-3 the length of right side is reduced to only 2 cm. They are evacuated from the left end by a TM pump of 500 l/s to a base pressure below 1×10^{-4} Pa. The operating gas is H_2 in this report at a pressure p_0 in the range of 2×10^{-2} to 5×10^{-1} Pa.

Microwave power P_μ up to 2 kW was applied using a magnetron in the continuous wave mode with a frequency of 2.45 GHz. An electron cyclotron resonance field of 875 G for the frequency of 2.45 GHz was applied by the two coils and the magnetic field gradient was controlled by the current Ic in the coils so as to move the resonance zone in z-axis along the magnetic flux.

Typical axial magnetic field distribution used in our experiment is shown in Fig. 1–4). The plasma was diagnosed by Langmuir probe, double probe, Farady cup (gridded energy analyzer, GEA)[5] and vacuum-ultraviolet (VUV) emission spectroscopy.

The electron temperature T_e and electron density n_e is determined with a Langmuir probe. Energy distribution of electrons and ions are measured with a gridded energy analyzer. The analyzer has a dimension of 5 cm in diameter and 4 cm in length. The front face has a hole of 5 mm diameter covered with a mesh of 0.2 mm wire separation. Transparency of the mesh is about 50%. The first, the second and the third grids have also the

† Received on May 8, 1989
* Associate Professor
** Graduate Student
*** Murata Seisakusho Co., Ltd.
**** Professor, Kansai University

Transactions of JWRI is published by Welding Research Institute of Osaka University, Ibaraki, Osaka 567, Japan

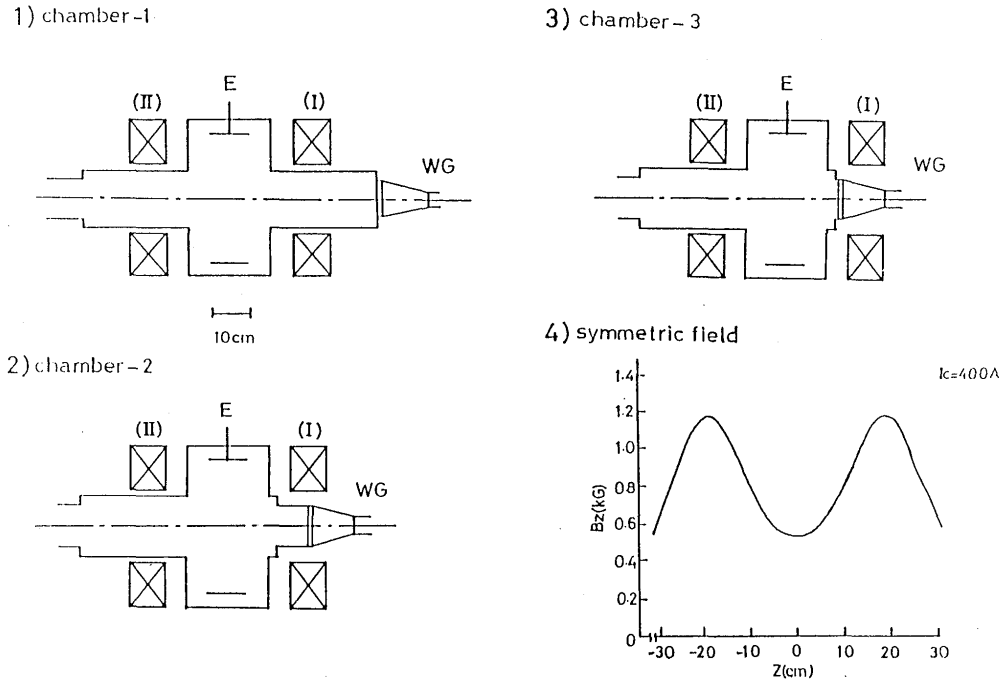

Fig. 1 Schematic diagram of experimental apparatus.

same hole size and mesh structure and the separation of each grid is set to be 7mm. The analyzer is inserted axially into the plasma and the energy distribution of particles parallel to the magnetic field is obtained.

The optical emission spectroscopy is applied in the VUV region. Observation is performed side on to the plasma flow. By a VUV spectrometer (the focal length of 20 cm) the emission in the range of 300A – 3000A can be detected with an inverse dispersion of 40A/mm.

3. Results and discussion

3.1 Plasma parameters in chamber-1

Property of the plasma in chamber-1 was studied by the measurement at the center of the plasma with the Langmuir probe. The electron temperature T_e did not change appreciably in comparison with the one by the chamber-2, even when several external parameters were varied widely. But the electron density n_e has showen a strong dependence on P_μ. Detailed results were described in a separate report[6].

3.2 Plasma property in chamber-2

We have examined plasma property and its spatial structure in the chamber-2. First electron temperature and electron density at the center of the plasma were measured by the probe as a function of the input microwave power P_μ and the current I_c of the magnetic coils as shown in **Fig. 2**. The electron temperature T_e clearly shows a strong dependence on the incident microwave power, especially in the case of I_c = 410A, The temperature

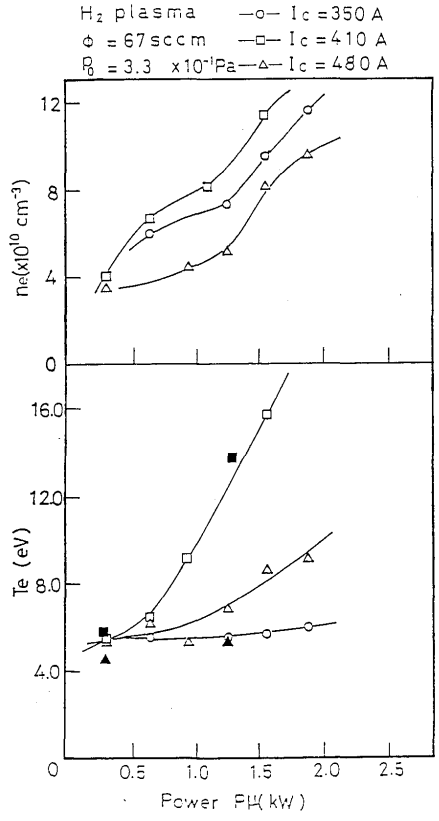

Fig. 2 Dependence of electron temperature T_e and density n_e on microwave power in various magnetic coil currents I_c measured at the plasma center. Black marks give the data by GEA.

is raised rapidly with increasing P_μ. The electron density n_e also shows a similar dependence with a higher value at I_c = 410A.

Figure 3 shows the axial distribution of T_e for various magnetic coil currents at $p_0 = 3.3 \times 10^{-1}$ Pa and $P_\mu = 0.46$ kW. The magnetic field has a symmetric mirror configuration with a mirror ratio of about 2 and the mirror throats are positioned at $z = \pm 19$ cm. We can clearly find a very strong non-uniformity in the axial temperature distribution. When the coil current I_c is 370A a strong peak in T_e appears with a value of about 18 eV at $z \simeq 12$cm. While at $I_c = 410$A the peak shifts to a position of $z \simeq 8$ cm with a lowered value of Te to about 14eV and at $I_c = 480$A this peak further shifts to $z \simeq 6$cm with a low temperature of about 8eV. These points are positioned a little inside of each resonance point at $I_c = 370$, 410, 480A on the axis. We note that other small peaks are observed in the region of $z < 0$cm. The shift of these peaks corresponds well to that of the resonance regions towards the center of the vacuum chamber and it seems that plasma production and heating is more efficient in the first resonance region positioned at $z > 0$, into which the wave is injected when the distance between the resonance zone and the wave input port at $z = 22$cm is smaller.

The higher the incident microwave power, the higher the temperature in the first resonance region. Meanwhile the data in Fig. 2 was obtained at the center of the plasma (i.e. on the midplane). In Fig. 3 T_e at $z = 0$ does not change appreciably at $P_\mu = 0.46$ kW for various values of I_c, which is nearly consistent with the data of Fig. 2. But when the input power is increased at $I_c = 370$A, T_e is drastically increased mainly in the resonance area that is away from the plasma center. While at $I_c = 410$A, the resonance region is nearer to the center and the temperature on the axis of the midplane can be higher than the case of $I_c = 370$A. When I_c is further increased to 480A T_e should be the highest, at the same power input, as the resonance region is closest to the plasma center. The heating rate, however, will become the least at $I_c = 480$A in comparison with other two cases, because the resonance zone is farthest from wave input port and the energy density is lowest due to the spread of the wave energy into the chamber area of 40 cm diameter. Thus T_e again decreases when compared with the case of $I_c = 410$A, as we have observed in Fig. 2.

We measured the axial temperature distribution in the case of the asymmetric magnetic field, where the current to the coil II is kept to be zero. The result is shown in

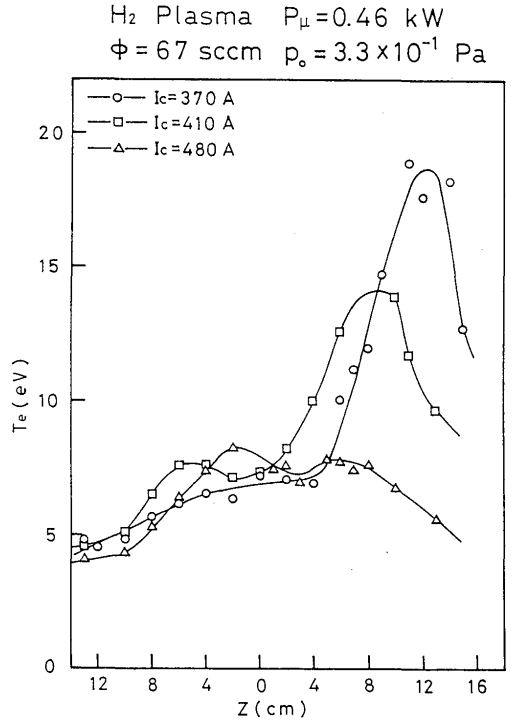

Fig. 3 Axial distribution of electron temperature for various magnetic coil currents.

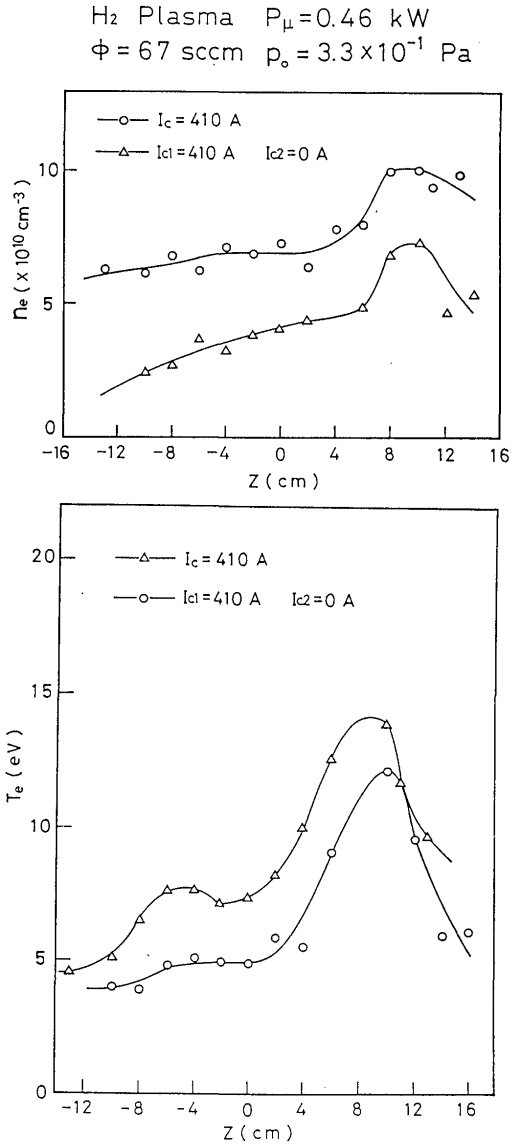

Fig. 4 Axial distribution of electron temperature and density in a symmetric and asymmetric mirror magnetic field.

Fig. 4. It has a similar variation with that in Fig. 3. But the temperature T_e and the density n_e are lower along the axis. This data was obtained in the condition of $p_0 = 3.3 \times 10^{-1}$ Pa, and the incident microwave power is considered to be absorbed almost in the first resonance region. So that the left resonance region gave little effect on the distribution in the symmetric field.

Figure 5 shows the pressure dependence of T_e and n_e for $P_\mu = 0.46$ kW measured at the center of the plasma making the field configuration again symmetric one. By varying the gas pressure, T_e rather than n_e is controlled appropriately.

Reducing the gas pressure to $p_0 = 9.3 \times 10^{-2}$ Pa and $p_0 = 2.4 \times 10^{-2}$ Pa, the axial distribution varies drastically as shown in **Fig. 6**. The distribution becomes more flat at $p_0 = 9.3 \times 10^{-1}$ Pa, but at $p_0 = 2.4 \times 10^{-2}$ Pa T_e becomes very high between the tow resonance region, and the peak of T_e in the resonance region disappears. This is because the collision in the plasma decreases in a lower gas pressure of 2.4×10^{-2} Pa and the incident microwave power is not absorbed in the first resonance region completely, by which also the second resonance region on the left side becomes efficient for the plasma production and heating.

The results mentioned above were obtained from the measurement with a Langmuir probe. We checked the variation of T_e using a gridded energy analyzer (GEA) and a good correspondence with the result by the Langmuir probe was obtained as shown by black marks in Fig. 2.

Furthermore we examined the result in Fig. 2 from VUV emission spectroscopy performed on the midplane

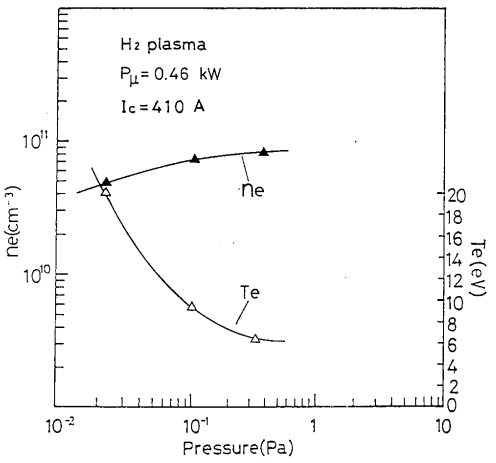

Fig. 5 Variation of electron temperature and density with gas pressure in the center of the plasma.

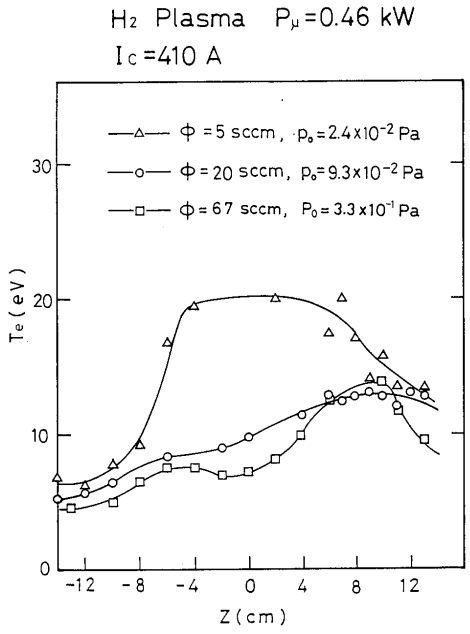

Fig. 6 Axial distribution of electron temperature and density for different gas pressures.

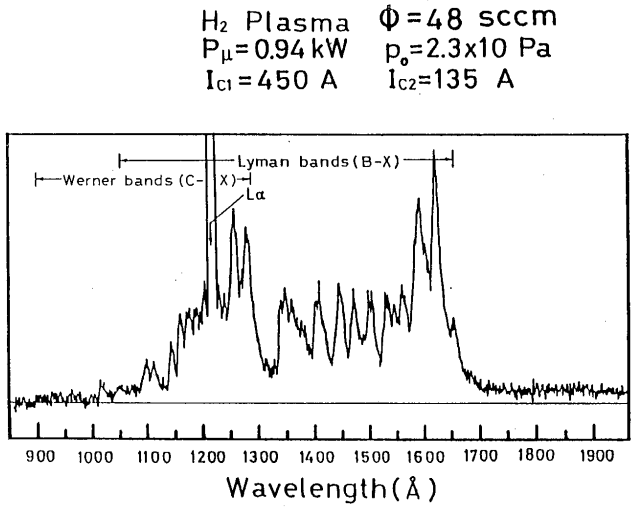

Fig. 7 A typical emission spectra of H_2 discharge in VUV range.

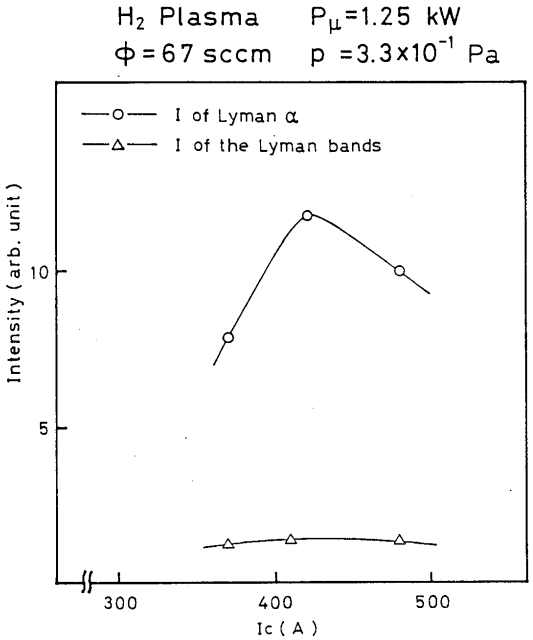

Fig. 8 Variation of intensity of Lyman line and of molecular line with different coil currents in the H_2 plasma.

of the plasma. Typical emission spectra is shown in **Fig. 7**. Various molecular spectra are obtained as well as atomic line of Lyman α of hydrogen[7–8]. **Figure 8** shows the variation of atomic and molecular lines with coil current I_c at P_μ = 1.25 kW and $p_0 = 3.3 \times 10^{-1}$ Pa. The intensity of Lyman α line exhibits a clear peak at a coil current of 410 A whereas the molecular line keeps nearly a constant value. This result corresponds well to the one obtained from the Langmuir probe in Fig. 2.

Figure 9 shows the distribution of T_e and n_e in the radial direction for different coil currents in the case of $p_0 = 3.3 \times 10^{-1}$ Pa. The electron density has nearly a flat distribution over $r > 10$ cm, while T_e varies appreciably with the change in I_c. This variation of the temperature distribution with I_c is considered to come from local heating process in the resonance region which differs spatially at each coil current

3.3 Plasma parameters in chamber-3

The configuration of chamber-3 is shown in the Fig. 1–3). As described already, the right side of chamber-3 was shortened to only 2 cm, so that the distance between the input port and the first resonance region becomes smaller in comparison with the case of chamber-2. **Figure 10** shows the axial variation of T_e in chamber-3 at the same external parameters with those of Fig. 3. In Fig. 10, however, the distance between the two coils are set to be about 36 cm, by which the resonance point at each coil current is positioned at a little smaller value of z in comparison with the case of Fig. 2. Indeed the distribution exhibits a similar spatial structure. As the input port of the microwave was closer to the resonance region on the right side, a more efficient heating inducing a higher T_e was expected to occur in the region of the resonance. The result, however, gives a T_e similar to or lower than that in Fig. 2. Thus we consider that the energy density of the incident microwave is different at the resonance regions corresponding to these coil currents. In the case of I_c = 480 A the resonance appears at $z \simeq 6$ cm, where the wave is distributed in a tube of 40 cm diameter. In Fig. 9 the wave in the resonance region at I_c = 480 A is also distributed in the chamber of 40 cm diameter ($z \simeq 4$ cm), by which the wave energy density at resonance is lowered remarkably in both cases giving a similar temperature distribution.

4. Conclusions

ECR plasma property in hydrogen gas was studied to be used for material processing. The following results were verified.

The electron temperature and electron density are higher in the resonance region of the ECR microwave plasma at a high gas pressure of around 10^{-1} Pa. Reducing the gas pressure to the range of 10^{-2} Pa the temperature becomes higher between the two resonance regions, indicating the bounce motion of heated electrons. Plasma parameters measured depend on the coil current strongly. By changing the coil current, the position of the temperature peak observed near the first resonance region is shifted in according with the shift of the resonance region in space. The plasma parameters measured at the plasma center could also be controlled by incident microwave power, gas pressure and coil current. These features

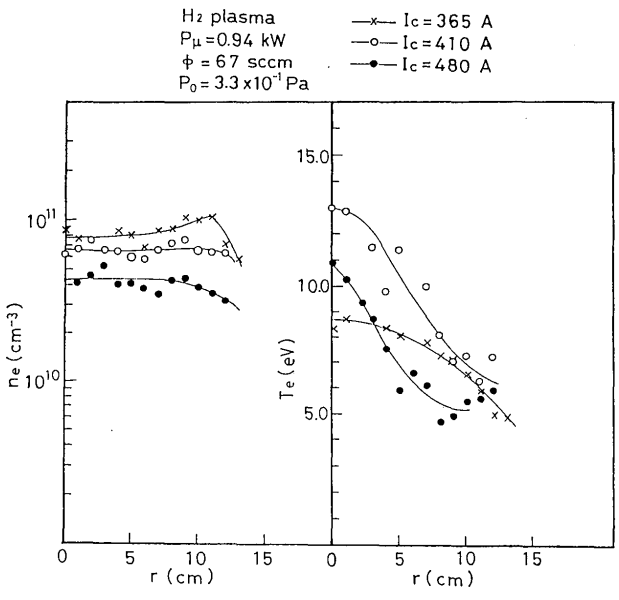

Fig. 9 Radial distribution of electron temperature and density for various magnetic coil currents.

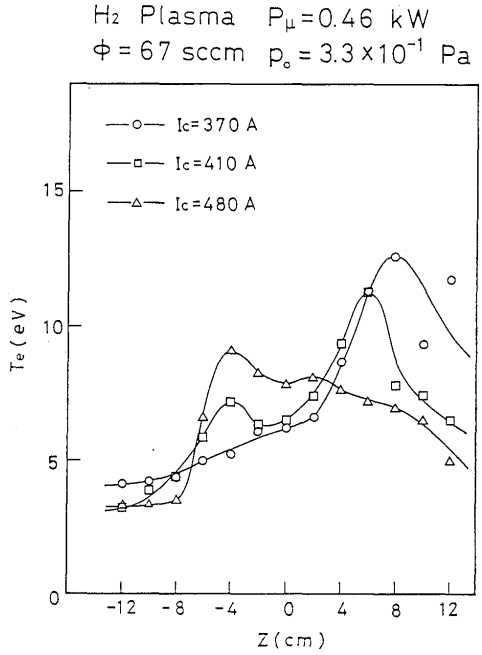

Fig. 10 Axial distribution of electron temperature for various magnetic coil currents in chamber-3.

should be estimated correctly in the optimum design of the plasma reactor and in performing various material processes.

Acknowledgment

The authors would like to thank Prof. Y. Arata, Kinki University for his interest and help to this work.

References

1) *Thin Film Processes,* edited by J.L. Vossen and W. Kern (Academic, New York, 1978).
2) *Deposition Technology for Films and Coatings-Development and Applications,* edited by R.F. Bunshah *et al.* (Noyes, Park Ridge, 1982).
3) S. Matsuo and M. Kiuchi, Jpn. J. Appl. Phys. Vol. 22, L210 (1982).
4) S. Matsuo, M. Kikuchi, and T. Ono, in *Proceedings of the 10th Symposium on Ion Sources and Ion-Assisted Technology* (ISIAT), Tokyo, 1986 (Ion Beam Engineering Experimental Laboratory, Kyoto University, Japan, 1986), p. 471.
5) J.L. Frankin, Stanley A. Stucniarz, and P.K. Ghosh, J. Appl. Phys. Vol. 39, No. 4 (March 1968), p. 2052.
6) S. Miyake, W. Chen, and Y. Shibata, in *Proceedings of 6th Symposium on Plasma Processing,* Kyoto, 1989, p. 12.
7) *Molecular Spectra and Molecular Structure,* edited by Gerhard Herzberg (D. Van Nostrand Company, Inc., 1950)
8) G. Herzberg and L.L. Howe, Can. J. Phys. Vol. 37 (1959), p 636.